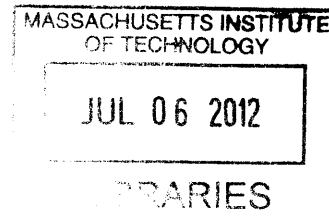


Dihydroazulene (DHA)

by Arathi Ramachandran

B.S. Materials Science and Engineering



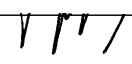
SUBMITTED TO THE DEPARTMENT OF MATERIALS SCIENCE & ENGINEERING IN
PARTIAL FULFILLMENT OF THE REQUIREMENTS FOR THE DEGREE OF
BACHELOR OF SCIENCE IN MATERIALS SCIENCE & ENGINEERING AT THE
MASSACHUSETTS INSTITUTE OF TECHNOLOGY

JUNE 2012

©2012 Arathi Ramachandran. All rights reserved.

The author hereby grants to MIT permission to reproduce and to distribute publicly paper and electronic copies of this thesis document in whole or in part in any medium now known or hereafter created.

Signature of Author: _____
Department of Materials Science and Engineering
Date

Certified by:  _____
Jeffrey C. Grossman
Professor of Materials Science and Engineering
Thesis Supervisor

Authorized by:  _____
Jeffrey C. Grossman
Professor of Materials Science and Engineering

Assessment of the accuracy of DFT (Density Functional Theory) for the Photochromic Behavior of
Dihydroazulene (DHA)

by Arathi Ramachandran

Submitted to the Department of Materials Science and Engineering on May _____ in Partial
Fulfillment of the Requirements for the Degree of Bachelors of Science in Materials Science and
Engineering

ABSTRACT

Efficient utilization of the sun as a renewable and clean energy source is one of the greatest goals and challenges of this century due to the increasing demand for energy and its environmental impact. Photoactive molecules that can store the sun's energy in the form of chemical bonds have been of interest to harness the sun's energy since the 1970s. However, all of the photoactive systems studied have problems with degradation making them impractical. Recently, the Grossman Group used computation to show that nanotemplating of the azobenzene photoactivesystem improves problems with degradation. We believe that this could be a platform technology for other photoactive systems like azobenzene. We would like to use high throughput screenings to identify other promising photoactive molecules. We would like to use Density Functional Theory (DFT) calculations for these studies, since DFT is the least computationally intense Quantum Mechanical model used on large chemical systems. For photosystems like azobenzene, norbornadiene, and diruthenium fulvalene, DFT predictions have been found to match well with experimental predictions, suggesting that DFT can be used to confidently predict properties of these fuels. However, for dihydroazulene(DHA) photoactive predictions using different DFT functionals do not match with each other and experiment. Our analysis suggests that lack of error cancelation due to a drastic change in the conjugation in DHA as compared to VHF might account for the variation in predictions based on different DFT functionals. It was also found that the DFT functional, ω B97X-D, makes similar predictions as the more computationally intense post Hartree-Fock methods by including couple cluster terms that better capture weak interactions.

Thesis Supervisor: Jeffrey C. Grossman
Title: Professor of Materials Science and Engineering

Table of Contents

| | |
|--|-----------|
| 1. Introduction | 5 |
| 1.1 Solar Thermal Fuels | 5 |
| 1.2 Previous Studies on the DHA/VHF System | 7 |
| 1.2.1 Experimental Studies | 7 |
| 1.2.2 Computational Studies | 9 |
| 2. Calculations | 10 |
| 2.1 Relaxed Structure Calculations | 10 |
| 2.2 Single Point Energy Calculations | 11 |
| 2.3 Hartree-Fock Methods | 13 |
| 2.4 Post Hartree-Fock Methods | 14 |
| 2.5 Density Functional Theory | 14 |
| 2.6 Error Cancellation | 17 |
| 2.7 Density Functional Theory Functionals | 18 |
| 2.8 Basis Sets | 20 |
| 3. Results and Discussion | 22 |
| 3.1 DHA/VHF Energy Calculations | 22 |
| 3.2 DHA/VHF Structure Calculations | 25 |
| 3.3 Visualization of Calculated Charge Density for DHA/VHF | 32 |
| 3.4 DHA/VHF HOMO LUMO gap Calculations | 33 |
| 4. Conclusions, Further Discussion, and Future Work | 35 |
| 5. Future Work | 38 |
| 6. References | 39 |

1. Introduction

1.1 Solar Thermal Fuels

Efficient utilization of the sun as a renewable and clean energy source is one of the greatest goals and challenges of this century due to the increasing demand for energy and its environmental impact. Numerous strategies exist to convert sunlight into useful forms of energy, including photocatalytic processes, artificial photosynthesis[1][2] photothermal power plants[3] and photovoltaic applications[4]. An alternative strategy to these is to convert and store the sun's energy directly in the chemical bonds of metastable photoisomers of suitable molecular systems. The stored energy can then be released as heat on demand by an external trigger. Ideally both the photoisomerization and heat release reactions reversibly occur in a closed-cycle without changing the chemical composition. The clear advantage of such an approach is that the same material both converts and stores the sun's energy, providing a rechargeable fuel that can be safely transported and used on-demand, the materials used could in principle be cheap, non-toxic and abundant, and the cycle can be repeated thousands of times without any emission or waste.

Many photoactive molecules that can convert the sun's energy into chemical bonds as shown in Figure 1.

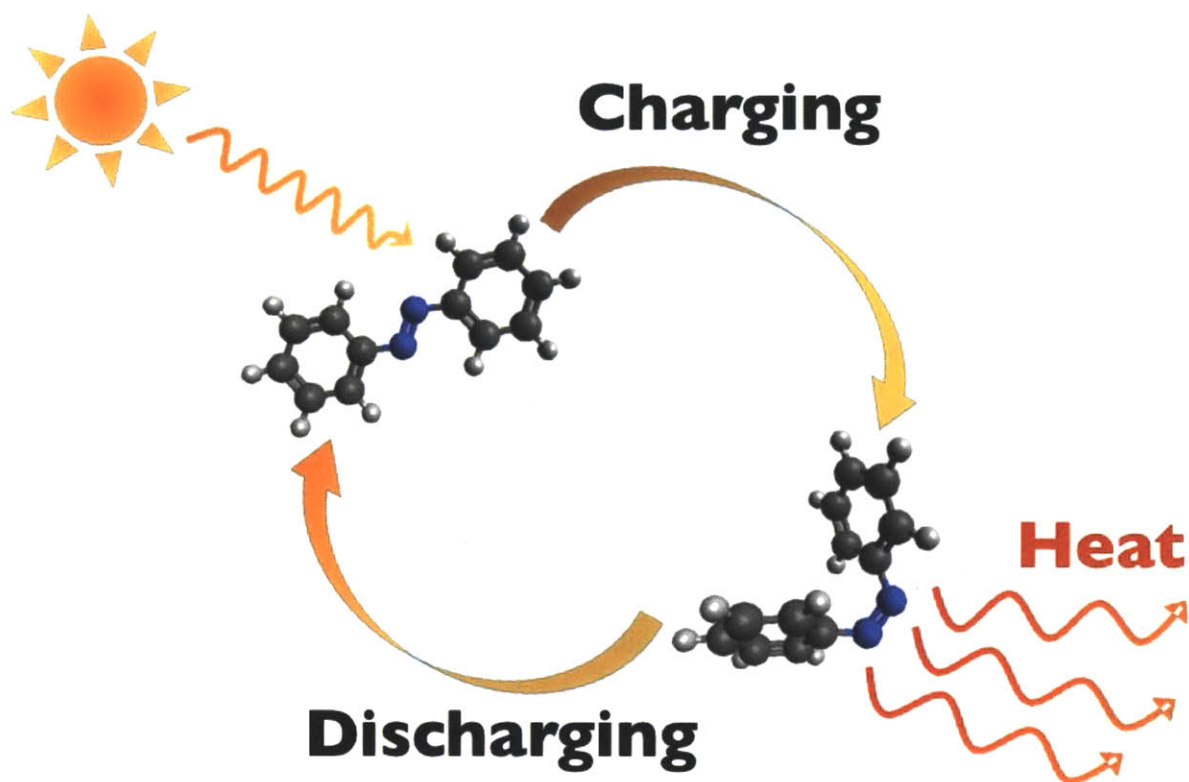


Figure 1. Mechanism for charging and Discharging Solar Thermal FUEls

However, these photoactive fuels or Solar Thermal Fuels are not practical to use due to high degradation rates upon cycling. The Grossman group have using the Quantum Computational method Density-Functional Theory(DFT), which is further discusses in the Calculations section, to show that carbon nanotube nanotemplating the azobenzene system improves the cyclability making it a practical Solar Thermal Fuel[5].Current experimental work underway in the group is bearing out this computationally driven solution.

There are many other photoactive molecules like azobenzene. We believe that this templating solution could improve the cyclability of these other systems as well. These photoactive systems were first studied in the 1980s when it was difficult to use quantum mechanical model to study large

chemical systems. Screening 100,000 photoactive fuels would have taken 30 years. Today due to improvements in hardware as well as the advent of methods like DFT, a screening of 100,000 fuels would take only 2 days.

In order to use DFT modeling to drive the design of these Solar Thermal Fuels, we would like to understand the limits of this method. For the azobenzene, norbornadiene, tetra-carbonyl-diruthenium fulvalene, and norbornadiene systems, Density Functional Theory (DFT) modeling predictions match experimental predictions closely ΔH [[5][6][7]. However, for the DHA/VHF system, different DFT functionals give significantly differing predictions about the stored ΔH , and do not match with observed experimental properties. This thesis compares the predictions of different DFT models with post-Hartree-Fock models of DHA/VHFs energy calculations and experimental calculations. We aim to discover which DFT functionals best capture the behavior of the DHA/VHF system, and what enables them to more accurately predict the enthalpy of reaction for the system. This Thesis will give further insight into when we would expect to trust different DFT calculations on these photosystems; and which functionals to use for problem systems like DHA/VHF.

1. 2 Previous Studies of DHA-VHF System

1.2.1 Experimental Studies

Dihydroazulene and vinylheptafulvene refers to the chemical structures shown in the reaction shown in Figure 2, where the R group varies. The photochemistry has been studied for R-groups of H, methyl (CH_3), cyanide (CN)[8], and Br[9] derivatives.

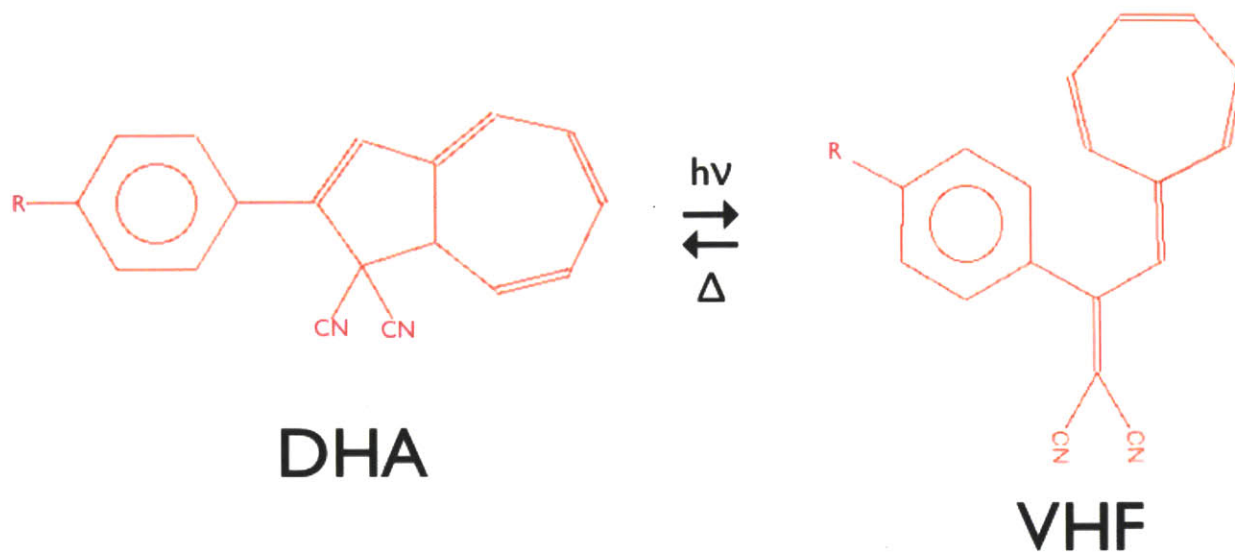


Figure 2. The ring opening DHA to VHF reaction and the thermal back reaction

There are published experimental structures for the CN[11] DHA and Br DHA derivatives[12]. Only one experimental structure was found for a methyl VHF derivative [10]. The ring opening reaction shown in Figure 2 occurs when DHA is illuminated with light of about 360nm [12],[10],[8]. No experimentally published values have been found for the enthalpy of the reaction¹. The thermal back-reaction was measured to have an activation energy of about 80kJ/mol(20kcal/mol) for each of these variants[12]. This back reaction can be facilitated by the addition of Lewis acids [13]. Both [8] and [9] took Ultra Violet/ Visible (UV/Vis) spectra for the both the CN[8] and Br derivatives of DHA and VHF while carrying out the ring opening and thermal reactions. They used this data to describe the kinetics system. The UV/VIS for the thermal back reaction for the CN derivatives for VHF to DHA are reproduced below in Figure 3. These spectra were used to compare to values found for the Highest Unoccupied Molecular Orbital (HOMO) Lowest Unoccupied Molecular Orbital (LUMO) gap for VHF and DHA. As shown in Figure 3, these spectra indicate that DHA has an absorption peak around

¹ Reference 6, which is in German, might have something about the thermochemistry, but I have not been able to decipher the paper. The paper also describes other reactions.

480nm and VHF has an absorption peak around 400nm [9] . Figure 3 also shows that DHA has an absorption peak around 360 nm, since we would expect to see an absorption peak at 360nm since the ring-opening reaction occurs for illumination of DHA with this wavelength of light.

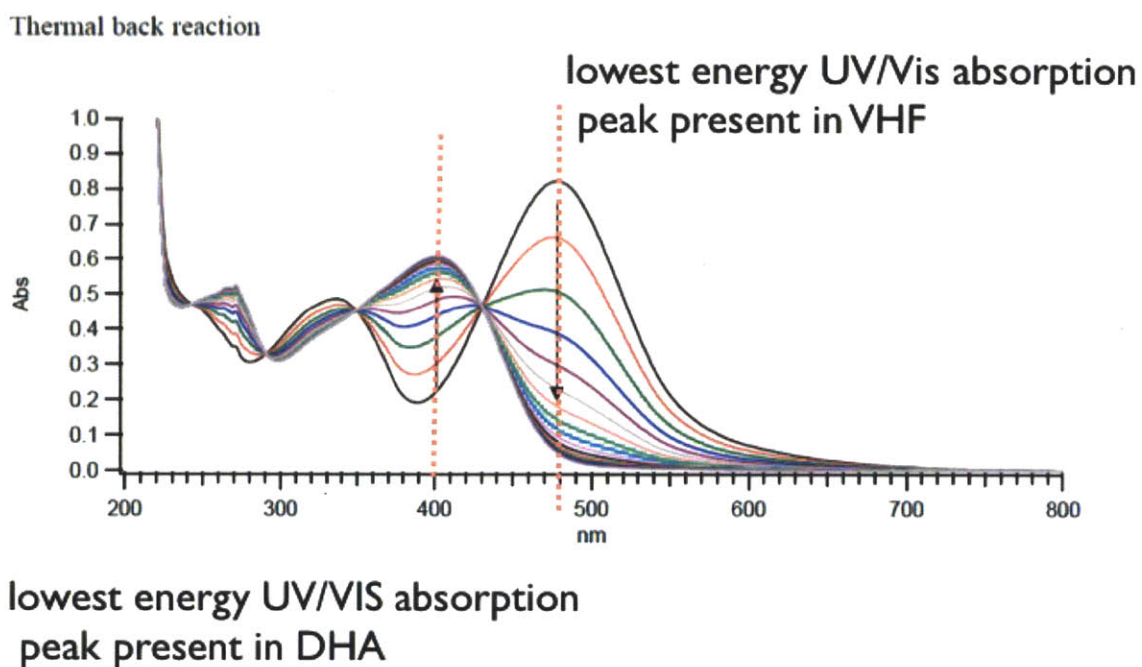


Figure 3. This Experimental Data and graph is taken from [8] for a kinetics experiment on the progress of the thermal reaction from VHF to DHA. The black curve is the UV/VIS spectra for the reactants, VHF, and grey curve is the UV/Vis spectra for the final product, DHA. The graphs indicate that VHF has a peak around 500nm and DHA has an absorption peak around 400nm

1.2.2 Previous Computational Studies

Boggio-Pasqua et al used complete active self consistent space field (CASSF) calculations to calculate a reaction profile for the DHA/VHF reaction[14]. They calculate an enthalpy of reaction of 10kcal/mol (40 kJ/mol) using CASSF calculations. CASSF calculations are a type of Hartree-Fock calculation that divides molecular orbitals in a molecule into active and inactive orbitals. Boggio-Pasqua et al also uses B3LYP DFT Functional with a Dunning-Basis Set and finds that DHA is 2 kcal more stable than VHF. Plaquet et. al calculated the geometries for DHA and VHF using B3LYP and 6-31G Pople basis set[15]

and used the Time Dependent Hartree-Fock (TDHF) equation to calculate the hyperpolarizability of the molecule. Placquet et. al suggest that this hyperpolarizability could be used in non linear optical applications.

2. Calculations

We calculated the enthalpy of the DHA-VHF back reaction by assuming that it's approximately equal to the difference in the internal energies of DHA and VHF. The internal energies of DHA and VHF were calculated by carrying out a relaxed structure calculation, which is further described in 2.1, using Density Functional Theory (DFT) and post Hartree-Fock(HF) methods. Both DFT and post- HF methods are ways of approximating the Time -Independent Schrödinger, Equation Eq. 1. In the Time-Independent Schrodinger Equation, \hat{H} is the Hamiltonian, which describes the energetics of the system, ϕ_i are the molecular orbitals of the system, and E is the energy associated with this molecular orbital.

$$\hat{H} \phi_i = E \phi_i \quad \text{Eq. 1}$$

For one electron systems like Hydrogen, He^+ , Li^{2+} etc., assuming a stationary nucleus, Eq.1 can be solved exactly. However, the Hamiltonian for a system with more electrons is non separable, and cannot be solved exactly. For systems like DHA and VHF the Hamiltonian that have many nuclei that each have many electrons either HF, Post-HF or DFT methods are needed to obtain approximate solutions to Eq.1 These methods are further described in Sections 2.3, 2.4, and 2.5 The Gaussian 09 Software Package was used to carry out all calculations[16]. The results were then visualized using Visual Molecular Dynamics (VMD) Software[17].

2.1 Relaxed Structure Calculations

The overall algorithm for solving for the geometry, wavefunctions, and energies associated with this

geometric and electronic configuration is shown in Figure 4. First an initial geometry is chosen, then Eq. 1 is solved using either Hartree-Fock or DFT models with a set of chosen basis functions. Then the electron density, which is the parameter in terms of which the Hamiltonian is written for these models, is checked against the initial chosen density until the density value converges. Then the position of the atoms are adjusted iteratively to obtain the lowest, converged energy configuration.

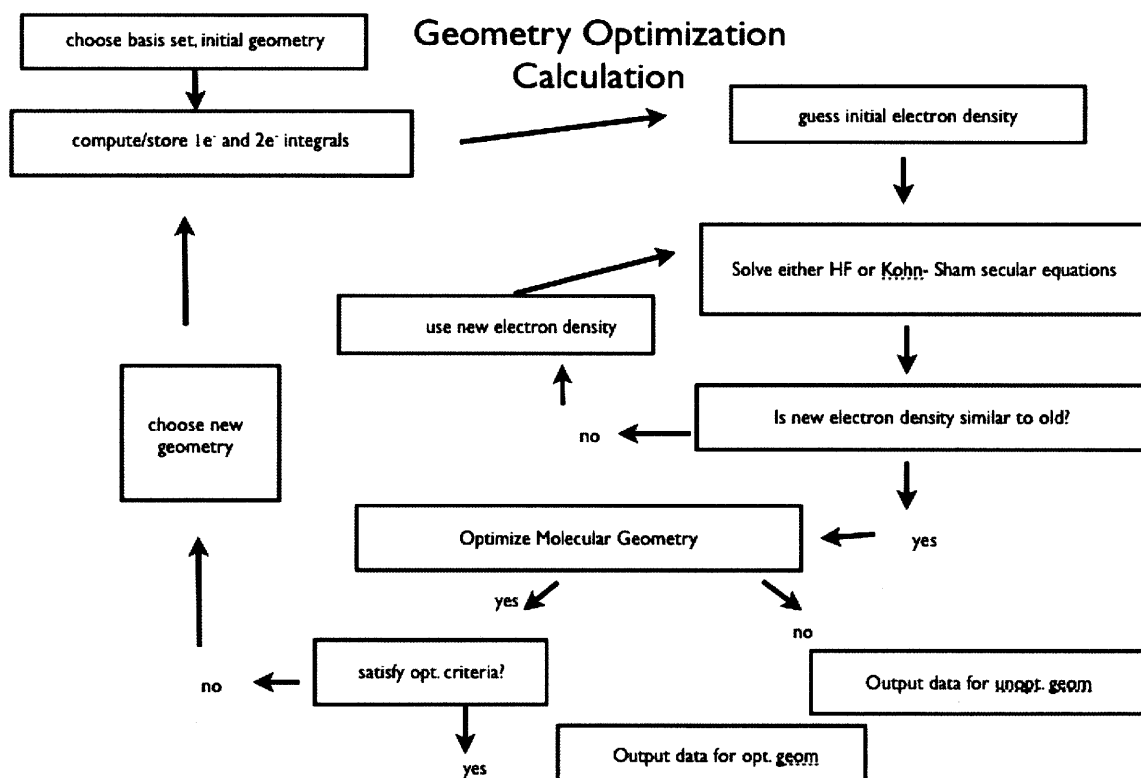


Figure 4. Schematic for Geometry Optimization Algorithm

2.2 Single Point (SP) Energy Calculations

The geometries for calculated relaxed structures might differ from the actual experimental structures, since the Hamiltonian used in all of these methods cannot exactly capture all the energy contributions of the system. One way we can assess this error is by carrying out a single point energy calculation for the experimental structure. For a single point energy calculation, the wave function and charge density, and energy are calculated for the given experimental geometry. You can imagine that a molecule has a Potential Energy Surface(PES) as shown in Figure 5, which represents the energy associated with any arrangement of the atoms, and that the actual experimental geometry of the molecule is a minimum associated with this system. The model of the molecule is given by another PES, which also has some minima, which represents the model's prediction of the molecules geometry. Ideally these two minima are the same. An SP calculation gives us an idea of how far apart these two minima are. SP Calculations for this system have been started.

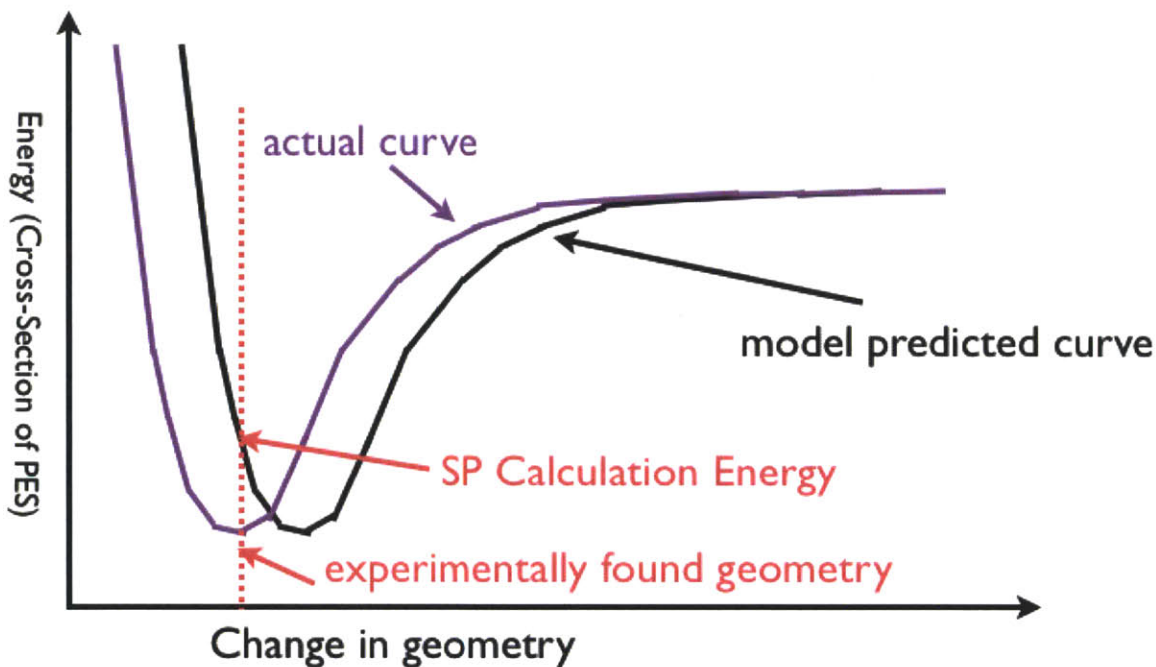


Figure 5. Single Point Energy Calculation

2.3 Hartree-Fock Methods

For a many-electron system, assuming that you have infinitely heavy point nuclei and can neglect spin-orbit interactions, \hat{H} , the Hamiltonian, is given by Eq. 2. In Eq. 2 \hbar is planck's constant divided by 2π , m_e is the mass of an electron, Z is the number of protons in the given atom, r_i is the distance between each electron and the nucleus, e is the charge of an electron, and r_{ij} is the distance between two different electrons.

$$\hat{H} = \frac{-\hbar^2}{2m_e} \sum \nabla_i^2 - \sum \left(\frac{Ze^2}{r_i} \right) + \sum \sum \frac{e^2}{r_{ij}} \quad \text{Eq. 2}$$

The first term in Eq.2, $\frac{-\hbar^2}{2m_e} \sum \nabla_i^2$ sums up the kinetic energies of each of the electrons around a given nuclei. The second term, $\sum \left(\frac{Ze^2}{r_i}\right)$ sums up the coulombic potential energy terms associated with each negatively charged electron being a distance r_i from a the positively charged nucleus. The third term $\sum \sum \frac{e^2}{r_{ij}}$ sums over the coulombic repulsive term between each pair of electrons about a nucleus. This equation is not separable due to the electron repulsion terms, which makes it impossible to solve exactly. Hartree-Fock methods solve Eq.1 and Eq.2 by initially guessing that the ground state wavefunction ϕ_0 about each atom in the system is a product of of basis set functions, like Slater Type Orbitals, which might be physically close to the actual ground state of the system. In order to account for spin, Hartree-Fock, also takes into account the spin-orbital operator, or Fock operator. Hartree-Fock often deals poorly with electron-correlation energy, or the energy associated with the fact that the behavior of electrons in a chemical system are not independent.

2.4 Post Hartree-Fock methods

Post Hartree-Fock methods improve on Hartree-Fock methods by attempting to take into account electron correlation energy. These methods use perturbation theory to improve upon the calculated ground state wavefunction ϕ_0 calculated using Hartree Fock. Couple Cluster(CC) Methods use the new guess, Ψ , as shown in Eq.3 to substitute back into the the Time-Independent Shrodinger Equation (Eq. 1). In Eq. 3 \hat{T} is the cluster operator defined in Eq. 4, and ϕ_i are the orbitals obtained from Hartree-Fock Methods.

$$\Psi = \sum e^{\hat{T}} \phi_i \quad (3)$$

$$\hat{T} = \hat{T}_1 + \hat{T}_2 + \dots \quad (4)$$

The cluster operator \hat{T} is the sum of the singlet operator \hat{T}_1 , the doublet operator \hat{T}_2 , etc. The singlet and doublet operators are defined in Eq. 5 and Eq. 6. t_i^a and t_{ij}^{ab} in Eq. 5 and 6 are constants that are solved for when the guess given in Eq. 4 is substituted back into the Time-Independent Shrodinger Equations. \hat{a} and \hat{a}^\dagger are the creation and annihilation operators. These creation and annihilation operators are analogous to the raising and lowering operators for the harmonic oscillator that operate on a given harmonic oscillator eigenfunction to give a lower energy eigenfunction and higher energy eigenfunction respectively. \hat{T}_1 and \hat{T}_2 convert a given orbital into a linear combination of singly excited and doubly excited Slater determinants.

$$\hat{T}_1 = \sum_i \sum_a t_i^a \hat{a}_i \hat{a}_a^\dagger \quad (5)$$

$$\hat{T}_2 = 1/4 \sum_{(i,j)} \sum_{(a,b)} t_{ij}^{ab} \hat{a}_i \hat{a}_j \hat{a}_a^\dagger \hat{a}_b^\dagger \quad (6)$$

Couple Cluster Singlet Doublet (CCSD) method is a CC method which includes singlet and doublet excited states. CCSD includes just the first two terms in Eq. 4. This method generally performs the best for estimating calculating the correlation energy of a system because it account for electron correlation in a physical manner.

Møller- Plesset (MP)Methods improve upon the the energy calculation by perturbing the Hamiltonian. Unlike CC methods, MP methods do not improve on calculation of the wave function. MP2, uses second order perturbations.

2.5 Density Functional Theory

Density Functional Theory(DFT) simplifies calculation by representing the Hamiltonian in terms of a functional, which is based purely on the charge density. The Hohenberg-Kohn Theorems justify the use

of DFT[18]. They show that a representation of the Hamiltonian in terms of a charge density functional exists that can be used to calculate the upper bound of the ground state energy. The Kohn-Sham Equations, which subsequent functionals discussed build upon, uses the assumption that each electron's behavior is independent to create such a functional. The Kohn-Sham Equations, Eq. 7, 8, and 9, are

$$\left[\frac{-\hbar^2}{2m} \nabla^2 + V_{system}(\vec{r}) \right] \phi_i(\vec{r}) = \epsilon_i \phi_i(\vec{r}) \quad (7)$$

$$V_{system} = V + \int \left(\frac{e^2 n_s(\vec{r}')}{|\vec{r} - \vec{r}'|} \right) d^3 r' + V_{XC} n_s(\vec{r}) \quad (8)$$

$$n_s(\vec{r}) = \sum_i |\phi_i(\vec{r})|^2 \quad (9)$$

where n_s is the charge density as a function of the position, \vec{r} the position, V the potential and kinetic energy of the system, and V_{XC} the exchange energy of the system. Eq. 7 is just a variation of the Time-Independent Shrodinger Equation or Equation 1 for each separable independent wave function ϕ_i for

each electron, where the first term in the operator $\frac{-\hbar^2}{2m} \nabla^2$ accounts for the kinetic energy of the electron, and the second term $V_{system}(\vec{r})$ takes into account other energy terms in the system. Eq. 8 and Eq. 9 allows for writing the Hamiltonian in Eq.7 in terms of a functional of the charge density. The main advantage of DFT is that it can be used to model larger systems than Hartree-Fock and Post Hartree-Fock methods, since calculations do not scale with the number of atoms in the system, but are dependent on the charge density. DFT however deals poorly with electron correlation energy because the Kohn-Sham equations used assume that electrons in many body system behave independently. Electron correlation energy is the energy associated with the correlated behaviors of electrons. In particular, these methods have difficulty dealing with long range forces like van der Waals attraction and pi-pi interactions. Both of these are present in our system. However, often error cancelation due to

similarities in the error involved in calculating the energy of the products and the reactants results in DFT obtaining fairly accurate calculations of the overall enthalpy of the reaction. DFT is also a lot less computationally intense than other methods of approximating Eq. 1.

2.6 Error Cancellation

According to Levine, HF and DFT energy calculations for light atoms can typically be in error by about 1/2% [15, pp. 315]. For Carbon, this is about 5 eV. The enthalpy values, that these models try to capture, however, are of this order. For many-systems, however the initial and final states are similar enough states that the errors cancel out in the enthalpy calculation. In order to further understand why error cancellation sometimes works, the error involved in calculating the enthalpy for different types of organic reactions has been studied. Pieniazek et. al studied the enthalpy of formation for Diels-Alder reactions [20]. These reactions involve the breaking of double bonds to form another single bond. An error build up for every time a double bond was broken was identified. Pieniazek et. al attribute this error to the fact that the electrons in the reactant are in pi bonding orbitals which are not present in the product. Pieniazek et. al refer to this as the $\pi \rightarrow \sigma$ transition. In the DHA/VHF system, the ring-opening results in a similar change in conjugation. DHA is made of three rings, where many of the p-orbitals on each of the Cs and Ns can interact. As a result, the bonding orbitals in DHA are fairly delocalized across the entire molecule. All of the calculations for both DFT and post Hartree-Fock methods for the charge distribution displayed this conjugated structure. In contrast, in VHF, the ring-opening reaction breaks the five-membered and results in the seven-membered ring being in a different plane from the phenyl ring. As a result, the p-orbitals in the seven membered ring cannot overlap with those in the rest of the molecule as easily. This means that the bonding orbitals that describe bonding in VHF are less delocalized than those that describe bonding in DHA. As a result, errors involved in predicting energies for orbitals present in VHF and for those present in DHA might not cancel. This might be why the

functionals looked at all give significantly different predictions for the enthalpy of the reaction. If this is the case, we would expect that functionals that handle weaker interactions like pi-pi interactions and van der Waals interactions will better model the system. This is because pi-pi interactions deal with bonding between adjacent p-orbitals like those present in the aromatic rings across DHA and in the phenyl ring in VHF. In molecules like DHA and VHF, which do not have a strong dipole moment, weak interactions like van der waals interaction often play an important role. Van der waals interactions deal with attractive interactions due to instantaneous polarization of the wave functions. This instantaneous polarization of the wave functions would involve excited state molecular orbitals. Since the p-orbitals involved in DHA can interact more easily with each other than in VHF, the higher energy molecular orbitals for DHA and VHF, which would be involved in these forces, probably look quite different. As a result, error for energy terms associated with these states might not cancel out in the enthalpy calculation.

2.7 DFT Functionals

DFT functionals have been developed in order to better account for correlation energies. These functionals improve upon the Kohn-Sham equations by changing the $V_{xc} n_s(\vec{r})$ term in Eq. 8, which takes into account the correlation energy, and exchange energy terms. Local Density Approximation (LDA) type functionals approximate the electron correlation and exchange energies as just functions of electron density everywhere in space. Generalized Gradient Approximation(GGA)functionals include a charge gradient term as well. Some Functionals are called meta-GGA functionals, which means that they include terms beyond the gradient of the charge density. Functionals can also treat spin-up and spin-down electrons separately. Some Functionals, like B3LYP try to write the exchange or correlation as a function of a parameter that describes the extent of electron interactions, which is obtained by

fitting empirical data. Some, like ω b97xd also optimized to correct for long- range interactions like van der Waals forces. The types of corrections added to the functionals are summarized in Table 1.

Table 1 Summary of the Energy Contributions, and Assumptions Part of the DFT Functionals Used

| Functional | Correlation Energy | Exchange Energy | Corrections for long range forces | Description of Principles of Construction |
|-----------------|--|--|---------------------------------------|--|
| LSDA | Uses local density corrections | Uses local density corrections | None | Treats system like a Homogenous Electron Gas (HEG) |
| PBE[21] | Uses non local density corrections | Uses non local density corrections | None | Improves upon HEG model by added non-local terms, which are parametrized by “fundamental constants” like a polarization, which has been optimized for Energy calculations of a number of systems. |
| PBE0[22] | Non-local PBE correction | exact HF exchange + non-local PBE correction | None | Adds some exact energy from the Hartree-Fock model to the pbe model to eliminate the polarization parameter in pbe optimized using spectral data |
| B3LYP | Non-local LYP correlation correction | Exact HF exchange+ Becke Exchange | None | Adiabatic Connection Method used in the Becke exchange term- this method was optimized for thermochemistry[23] applications LYP uses the electron density and a laplacian of the second order Hartree-Fock Density Matrix to calculate electron correlation energy[22, pp. 268] |
| τ PSSh[25] | Meta GGA correction of PKZB functional(similar to PBE functional) | Meta GGA correction | None | same basic principle as PBE functional just adds terms beyond the gradient of the charge density. |
| ω B97X-D | Local correlation corrections | Exact HF exchange + Local corrections | Long-Range Corrected (LC) Functional | LC Functional to indicate that the coulomb potential is partitioned such that for large inter-atomic distances configuration interaction terms are included[26],[27] |

2.6 Basis Sets

The Molecular orbitals, Φ_i , in the time independent Schrodinger Equation (Eq. 1), are expressed in terms of Basis Functions χ_r , as shown in Eq. 8

$$\phi_i = \sum_r c_{ri} X_r \quad (8)$$

These Φ_i , need to be expressed in terms of basis functions, since the eigenfunctions for the Schrodinger equation for system are not known. Eventually, for a large number of basis functions, this expansion should converge to desired molecular orbital. Two types of basis sets were used: 1) the Pople basis functions and 2) the Dunning basis functions. Terminology used to describe basis functions are described in the following discussion. Slater Type orbitals and Gaussian Type orbitals are considered minimal basis sets, since they crudely describe the orbitals. Split valency basis sets use one function for core orbitals and more functions to describe the behavior of valence orbitals. Double-zeta, triple-zeta, quadruple, etc. are split valency basis sets that use two, three, four, etc. different functions in the valence orbital description from those used in the core orbital description. Polarization functions allow the p,d, etc. angular momentum components to change. Diffuse functions are broad gaussian functions used to capture the tail end behavior of an orbital. The basis functions used are summarized in Table 2.

Table 2: Basis Sets Summary

| Basis Sets | Description |
|--------------------------------------|--|
| Pople Basis Functions | |
| 6-31G | -Uses 6 functions to describe core shell orbitals - triple-zeta basis set, so it uses an extra three functions to describe valence orbitals |
| 6-31G(d,p) | -same as 6-31G description with added d and p polarization functions |
| 6-311G(2d,d,p) | -same as 6-31G description with added 2d, d and p polarization functions |
| 6-311+G(2d,d,p) and 6-311++G(2d,d,p) | -same as 6-311G(2d,d,p) description but includes diffuse functions as well |
| Dunning Basis Functions | |
| cc-pVDZ | A double-zeta type basis set with added polarization functions. |
| cc-pVTZ | A triple zeta type basis set with added polarization functions. |
| aug-cc-pVTZ | A triple zeta type basis set with added polarization functions, and added diffuse functions. |

For the pople basis functions, the first number before the dash represents how many functions are used to describe the core orbitals. The number after the dash describes whether the basis function is a double-zeta, triple-zeta, etc. functional. The Dunning Basis Set Functions were optimized for configuration interaction calculations, which is indicated by the cc. The p indicates that polarization functions are included. VDZ, TDZ, 4DZ, etc. refer to whether the basis set is a double-zeta, triple-zeta, quadruple-zeta, etc. basis set respectively. The added aug at the front of the basis set description shows that diffuse functions are included.

All of the results displayed, except for the CCSD and M06 calculations use basis sets for which the energy had converged. Convergence is assessed based on whether the energy stays the same for the

addition of more basis functions. Convergence for the B3LYP calculations is shown in Figure 6 as an example.

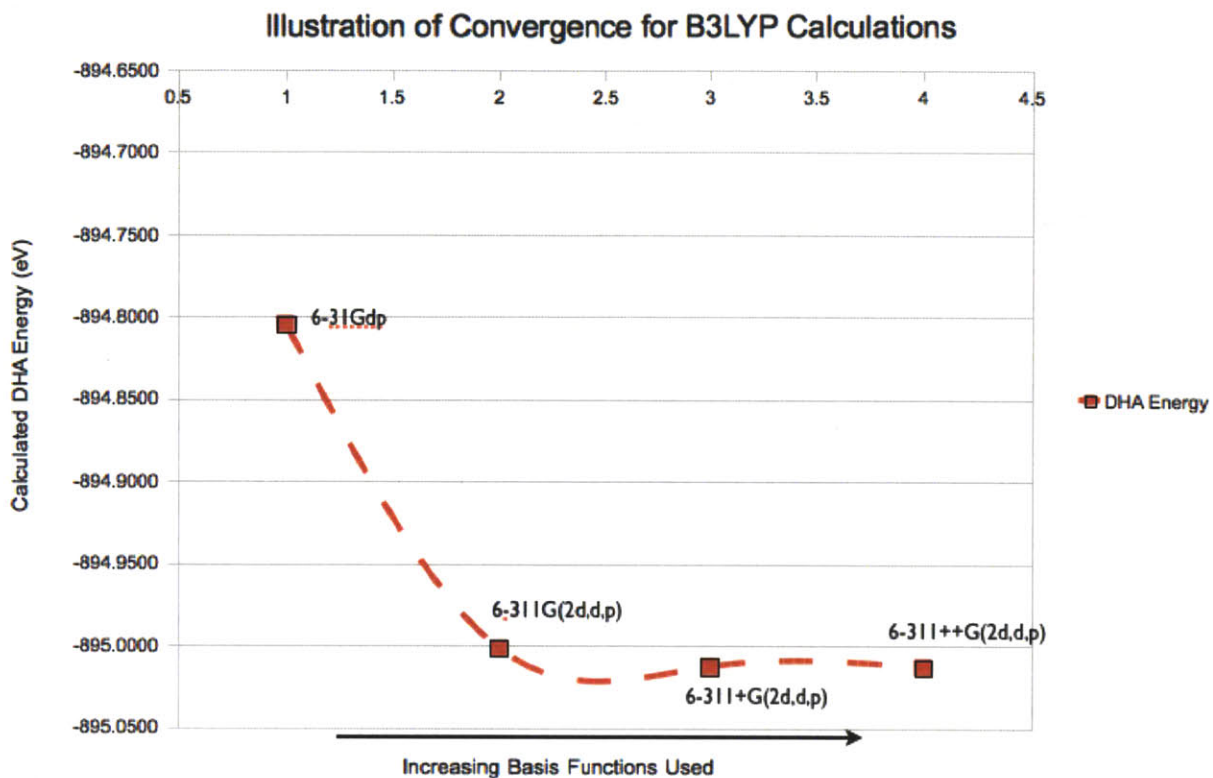


Figure 6. Illustrates convergence of energy calculations for DHA for B3LYP. All the results for methods shown use a converged basis set.

3. Results and Discussion

3.1 DHA/VHF Energy Calculations

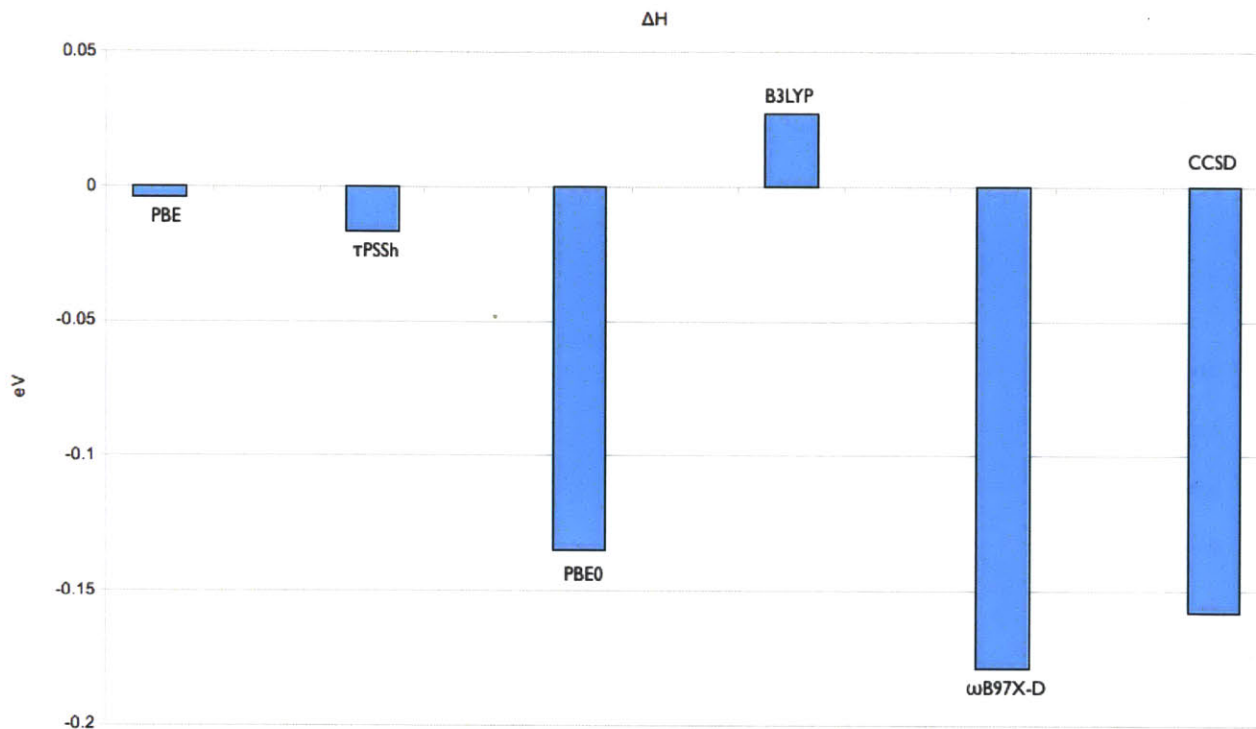


Figure 7: Shows the enthalpy calculations for each of the DFT methods

Figure 7 shows that all the DFT and post-Hartree-Fock methods used predict significantly different enthalpies for the DHA/VHF system. B3LYP is the only system that predicts an endothermic back reaction. It is known that this system acts as a thermoswitch, so this calculated enthalpy must be inaccurate. This is worrying, since B3LYP is the standard method used by most quantum chemists. Since B3LYP is a hybrid functional that uses the LYP functional in addition to an empirically fitted exact exchange, it would be interesting to see how the LYP functional performs. It's interesting to note that the PBE, PBE0, and τPSSh give such different ΔH calculations, since both PBE0, and τPSSh are variants of PBE. Both PBE0, and τPSSh use a different parametrization of the correlation and exchange energy in terms of a polarization constant, which they claim is universal to all chemical systems[22] [25]. Tao et al even claims that these methods should nest within each other for different levels of calculation[25]. The ωB97X-D functional calculations and the CCSD calculations arrive at similar ΔH .

This might be due to the fact that the ω B97X-D functional partitions the Hamiltonian such that for certain configurations CC terms are included in the calculation. It will be interesting to note if this trend holds for larger basis set CCSD calculations on the system.

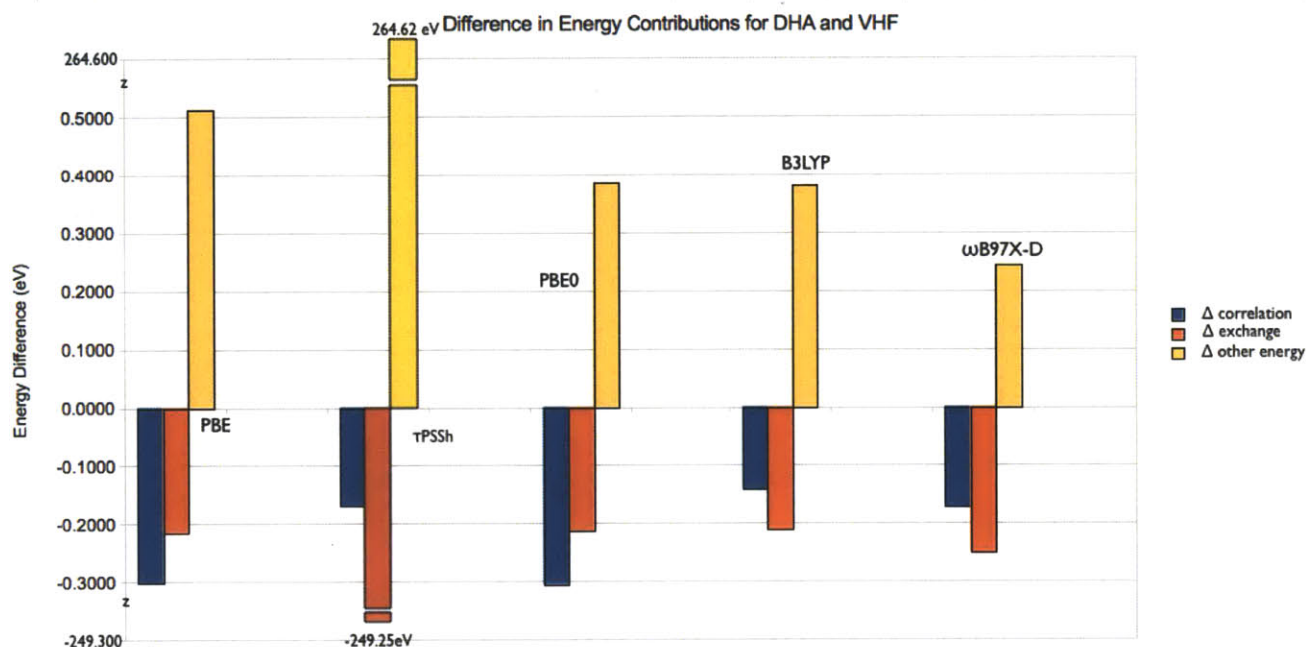


Figure 8. Shows the differences in the correlation, exchange, and other energy term contributions to the internal energy calculations of DHA and VHF. The red bar is the exchange energy, the yellow the correlation, and the blue is all the other contributions.

Looking at Figure 8, for all of the methods, except τ PSSh, the exchange-energy, and other energy calculations for DHA and VHF seem to be similar. For the τ PSSh calculation of the system, the VHF calculation seems to have significantly more of an exchange energy and significantly less other energy contributions than the DHA exchange energy contribution and other energy contribution respectively. The exchange energy difference (264.62 eV) and other energy contribution (-264.47 eV) differences between VHF and DHA for τ PSSh calculation almost exactly cancel, suggesting that in this system, perhaps these two energies aren't decoupled in the manner that the Hamiltonian for this model suggests. If all of the functionals are predicting the same structures for VHF and DHA, you would expect the

same difference in other energy, since the energy contributions other than the correlation and exchange energy are the potential and kinetic energies. Each of the functionals seems to have quite different energy contributions from these terms

3.2 DHA/ VHF Structure Calculations

Table 3: Comparison of DHA Experimental Structure(Shown in Figure 9 with labeled atoms) Bond Lengths and Angles [22] with Calculated Bond Lengths and angles

| | Experimental Bond Lengths(Å) | CCSD (6-31G)(Å) | ω B97X-D (Pople Basis)(Å) | PBE0 (Pople Basis)(Å) | PBE (Dunning Basis)(Å) | τ PSSh (Pople Basis)(Å) | B3LYP (Pople Basis)(Å) |
|------------|------------------------------|-----------------|----------------------------------|-----------------------|------------------------|------------------------------|------------------------|
| C1–C8a | 1.57Å | 1.57 | 1.58 | 1.58 | 1.59 | 1.59 | 1.59 |
| C1 – C15 | 1.48 | 1.49 | 1.47 | 1.47 | 1.47 | 1.48 | 1.47 |
| C1 – C16 | 1.48 | 1.50 | 1.47 | 1.47 | 1.47 | 1.48 | 1.47 |
| C2 – C9 | 1.46 | 1.49 | 1.47 | 1.46 | 1.46 | 1.46 | 1.46 |
| C1–C2 | 1.55 | 1.57 | 1.54 | 1.54 | 1.55 | 1.55 | 1.55 |
| C2–C3 | 1.35 | 1.36 | 1.34 | 1.35 | 1.36 | 1.36 | 1.35 |
| C3–C3a | 1.43 | 1.43 | 1.45 | 1.43 | 1.43 | 1.44 | 1.43 |
| C4–C3a | 1.34 | 1.36 | 1.35 | 1.36 | 1.37 | 1.37 | 1.35 |
| C4–C5 | 1.44 | 1.47 | 1.44 | 1.43 | 1.43 | 1.44 | 1.43 |
| C5–C6 | 1.34 | 1.37 | 1.36 | 1.36 | 1.37 | 1.38 | 1.36 |
| C6–C7 | 1.44 | 1.48 | 1.45 | 1.44 | 1.43 | 1.44 | 1.44 |
| C7–C8 | 1.34 | 1.36 | 1.34 | 1.34 | 1.35 | 1.36 | 1.34 |
| C8–C8a | 1.50 | 1.53 | 1.50 | 1.50 | 1.50 | 1.51 | 1.50 |
| C8a–C3a | 1.51 | 1.54 | 1.51 | 1.51 | 1.51 | 1.52 | 1.51 |
| | Experimental Bond Angles | | | | | | |
| C2–C1–C8a | 104.32° | 103.90° | 104.23° | 104.41° | 104.37° | 104.43° | 104.19° |
| C1–C2–C3 | 108.53 | 110.14 | 109.53 | 109.12 | 108.75 | 108.91 | 109.07 |
| C2–C3–C3a | 113.43 | 112.63 | 112.84 | 110.12 | 113.67 | 113.39 | 113.79 |
| C3–C3a–C8a | 108.72 | 108.80 | 108.87 | 109.17 | 109.42 | 109.39 | 109.19 |
| C4–C3a–C8a | 122.13 | 123.08 | 123.08 | 122.87 | 123.01 | 122.84 | 123.42 |
| C3a–C4–C5 | 124.43 | 124.28 | 124.31 | 124.74 | 125.58 | 125.07 | 125.51 |
| C4–C5–C6 | 125.75 | 125.65 | 125.63 | 125.85 | 126.16 | 126.06 | 126.20 |
| C5–C6–C7 | 125.94 | 126.04 | 126.01 | 125.90 | 125.97 | 126.00 | 126.20 |
| C6–C7–C8 | 125.44 | 125.90 | 126.05 | 126.25 | 126.81 | 126.49 | 126.87 |
| C7–C8–C8a | 120.73 | 120.72 | 120.65 | 120.87 | 121.58 | 121.05 | 121.73 |
| C8–C8a–C3a | 107.92 | 109.50 | 108.12 | 108.08 | 108.73 | 108.50 | 109.48 |
| C1–C8a–C3a | 103.42 | 103.55 | 103.37 | 103.47 | 103.49 | 103.35 | 103.45 |

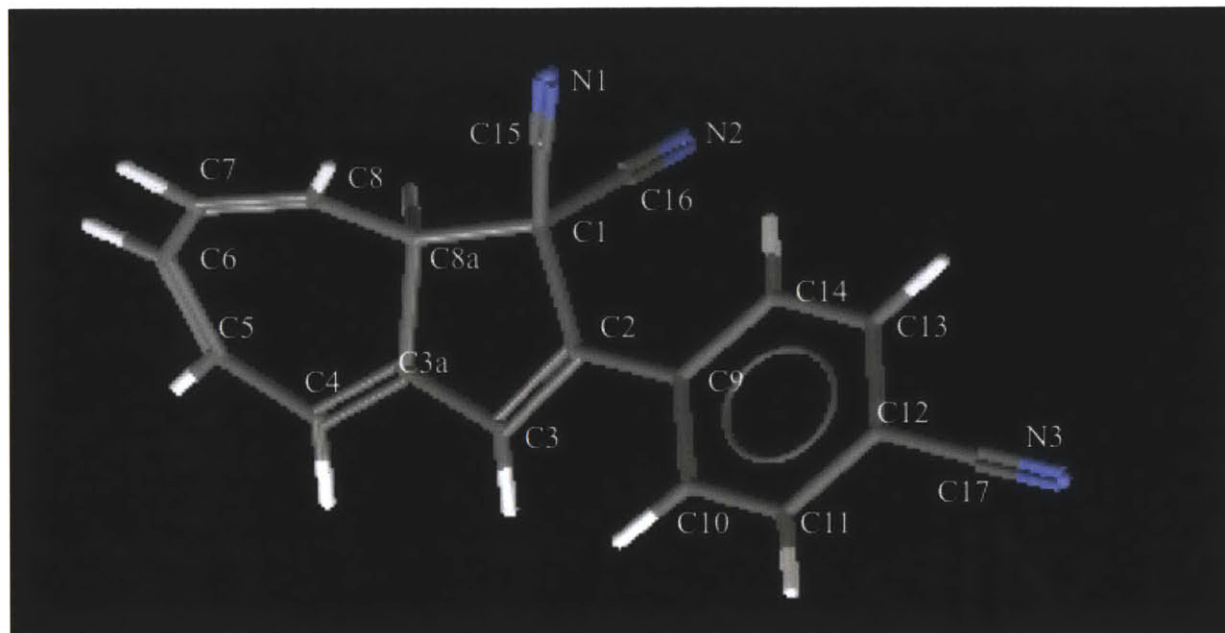


Figure 9. Experimental Structure for DHA from [11] Visualized using Cambridge Structural Database's (CSD's) Mercury Analysis Software

Comparing the values in Table 3 for the bond lengths and angles in DHA in the seven-membered and five membered rings shows that all the methods used for calculating structure of DHA calculate the bond length and bond angles to within 0.03\AA and 1° of the experimentally quoted values, which suggests that all methods explored calculate the geometry reasonably well.

Table 4: Comparison of Calculated VHF Structures

| Method | Out of Plane Distortion in VHF (measured by taking the distance between the two carbons labeled in Figure 10) |
|-------------------------------|---|
| CCSD (6-31G) | 2.56 \AA |
| ω B97X-D (Pople Basis) | 2.39 \AA |
| PBE0 (Pople Basis) | 2.55 \AA |
| PBE(Dunning) | 2.57 \AA |
| TPSSh (Pople) | 2.56 \AA |

| | |
|--------------|-------|
| B3LYP(Pople) | 2.56Å |
|--------------|-------|

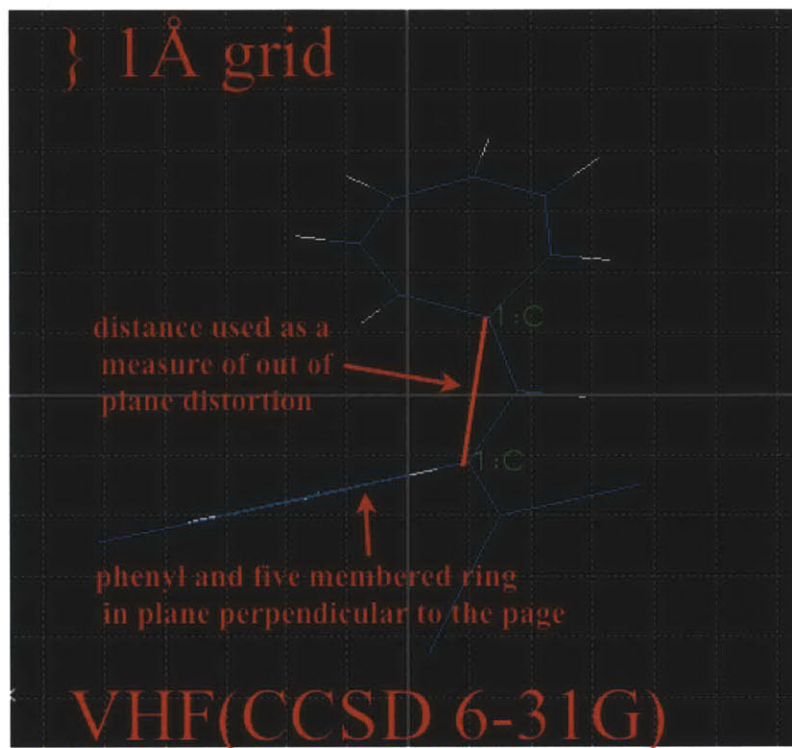


Figure 10. The distance between the two carbons labeled on the structure calculated for VHF were used to measure the out-of-plane distortion calculated for VHF for each method as displayed in Table 4

As shown in Table 4, the out-of plane distortion in VHF calculated for all methods, except ω B97X-D, was around 2.55 to 2.57 Å. The ω B97X-D functional predicted an out-of plane distortion of 2.39 Å, which is significantly smaller. This suggests that this functional predicts a significantly different geometry from the other functionals. This functional tries to take into account long-range forces such as van der Waals interactions by including higher order Couple cluster terms for large distances between atoms. One hypothesis for this smaller distance could be that this functional is accounting for some interaction between the two CN groups and the seven-membered ring. If this hypothesis is correct, you

would expect all of the methods to calculate the same distance between the two labeled carbons if the seven membered ring was replaced with a methyl group. Comparison of the energy contributions to the enthalpy calculation (Figure 8) shows that calculated potential energy and kinetic energy terms differed for each of the methods. One explanation for this observation is that the functionals all give different structure predictions for DHA and VHF. The structure calculations, show that all functionals calculate structures for DHA that agree reasonably well with experiment. This does not explain the observation that the potential and kinetic energy contributions to the energy calculation are different for each method. It seems as though different functionals calculation of the structure of VHF might not agree as well. Experimental structures for this derivative of VHF have not been found. However, experimental structures for a methyl derivative of VHF have been found[10]. Investigating how calculations for this structure by the different functionals might give better insight into this observation.

3.3 Visualization of Charge Distribution in DHA and VHF

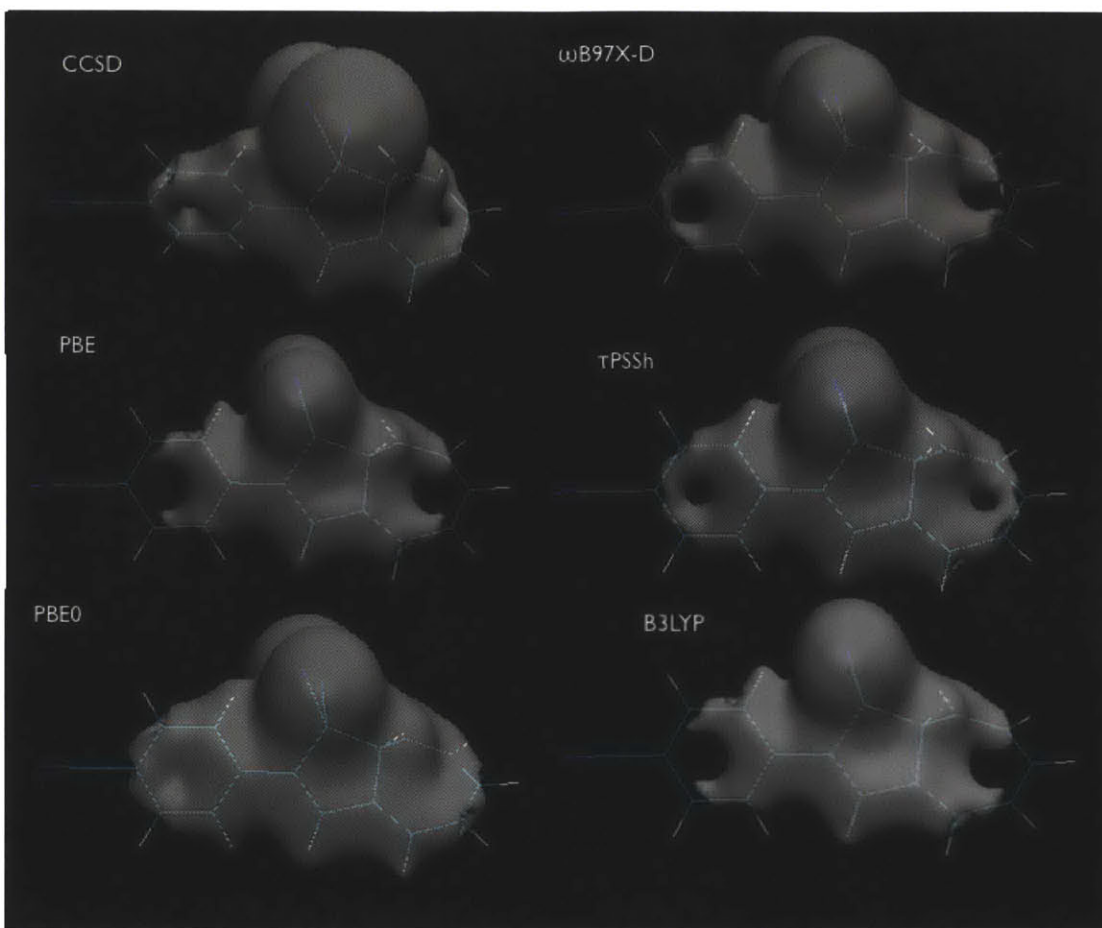


Figure 11. VMD Visualization of Charge Distribution in DHA as calculated by each of the methods

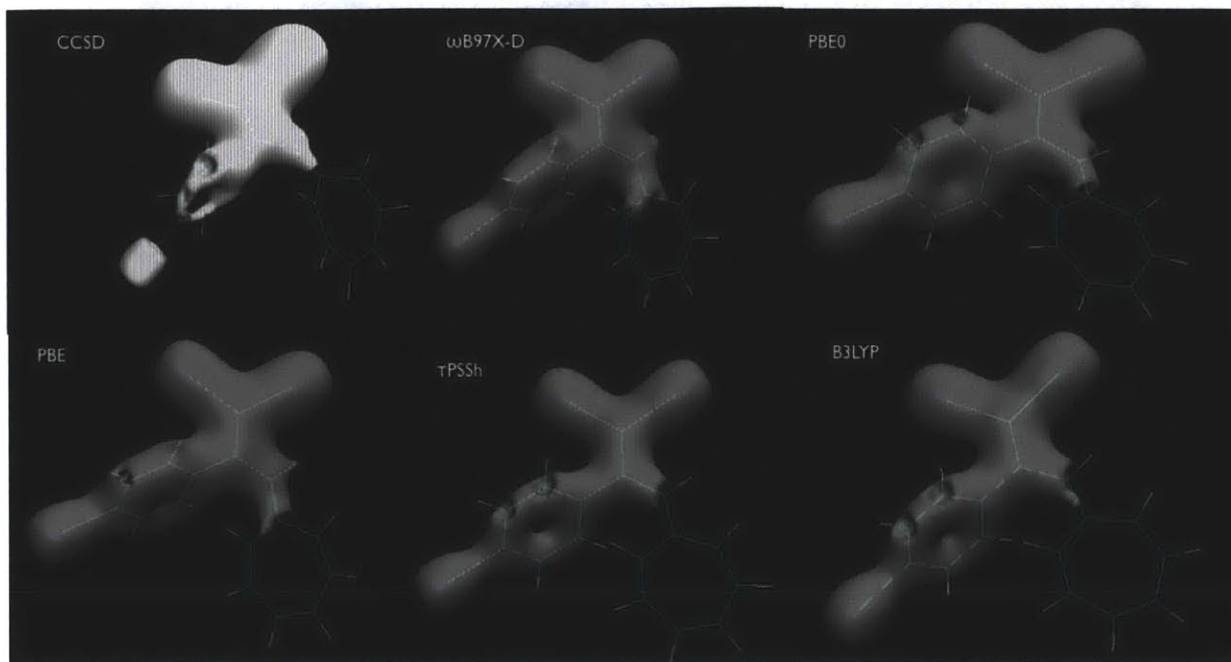


Figure 12. VMD Visualization of Charge Distribution in VHF as calculated by each of the methods

Figures 11 and 12 show that all methods show that the ring opening reaction results in a break in conjugation. Rather in DHA, the whole structure is conjugated, while In VHF, the out-of-plane distortion causes the seven membered ring to not interact with the pi orbitals in the phenyl ring and the CN groups. All of the functionals also show that the strong electron withdrawing CN groups have a significant effect on the charge distribution. In DHA, the two CN groups attached to the five-membered ring seem to draw much of the charge, while the CN group on the phenyl ring does not have a large population of charge concentrated around it. In the VHF structure, all three CN groups seem to have charge clustered around them. It would be interesting to compare how these calculations compare to calculations for the Br derivative of the DHA/VHF system, since Br is a less strong electron withdrawing group.

3.4 DHA/VHF Highest Occupied Molecular Orbital(HOMO) Lowest Unoccupied Molecular Orbital (LUMO) Gap Calculations

UV/Vis Spectra for DHA and VHF shows that DHA has an absorption peak around 400nm, which would correspond to about a 3 eV transition, and VHF has an absorption peak around 500nm, which corresponds to about a 2.5 eV transition. The calculated HOMO LUMO gap for DHA and VHF are shown in Figures 13 and Figures 14 respectively. The methods predict a gap for VHF and DHA that varies between 1eV and 5eV and .9eV and 4eV respectively. This variation in predicted HOMO LUMO gap is large. The ω B97X-D DFT functional and the MP2 both overestimate the gap, while the other methods under estimate the gap. One hypothesis for this could be that perturbative methods overestimate tend to overestimate the energy for a given eigenstate. MP2 is a perturbative method, and the ω B97X-D DFT functional includes CC terms. Perturbation is used in calculating these CC terms. It

would be interesting to compare whether CCSD calculations also overestimate the gap. We could also look at whether these same methods overestimate and underestimate other absorption peaks shown in Figure 3 for DHA and VHF.

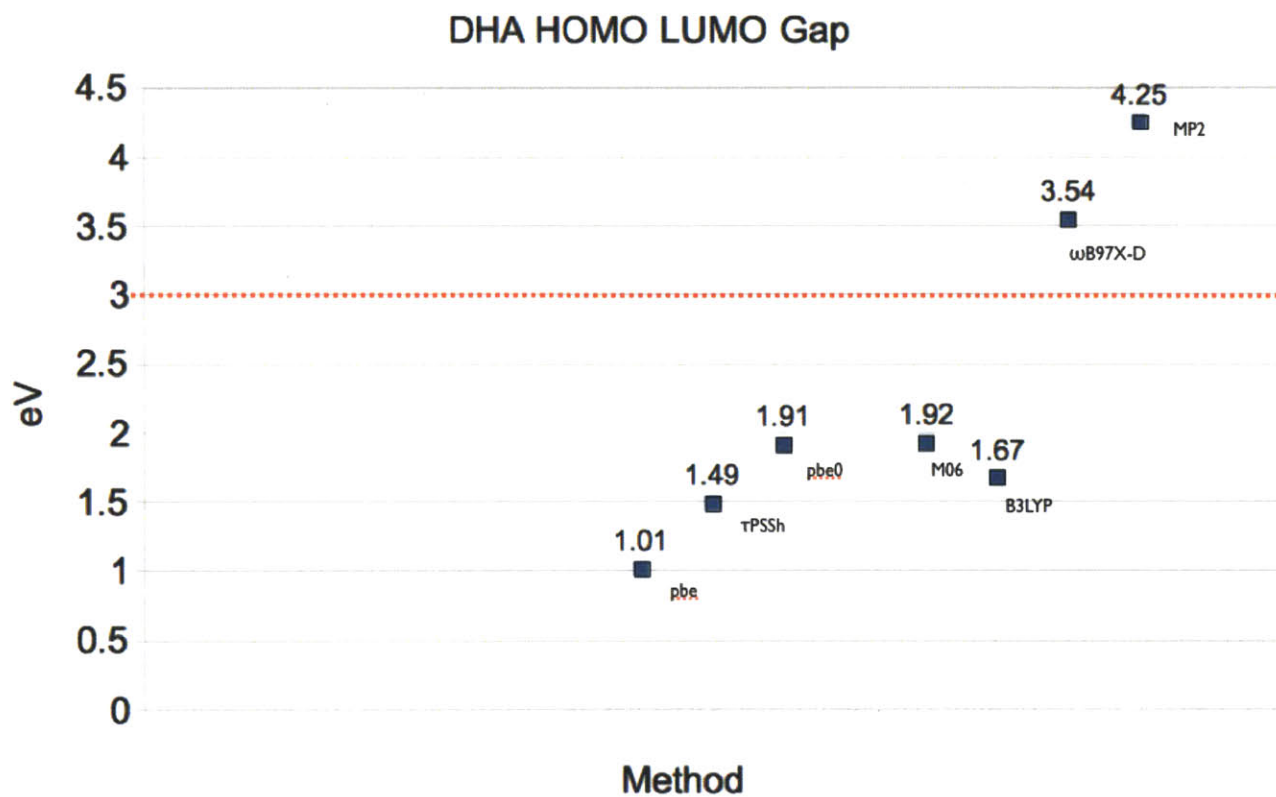


Figure 13. Calculated HOMO, LUMO gap for DHA

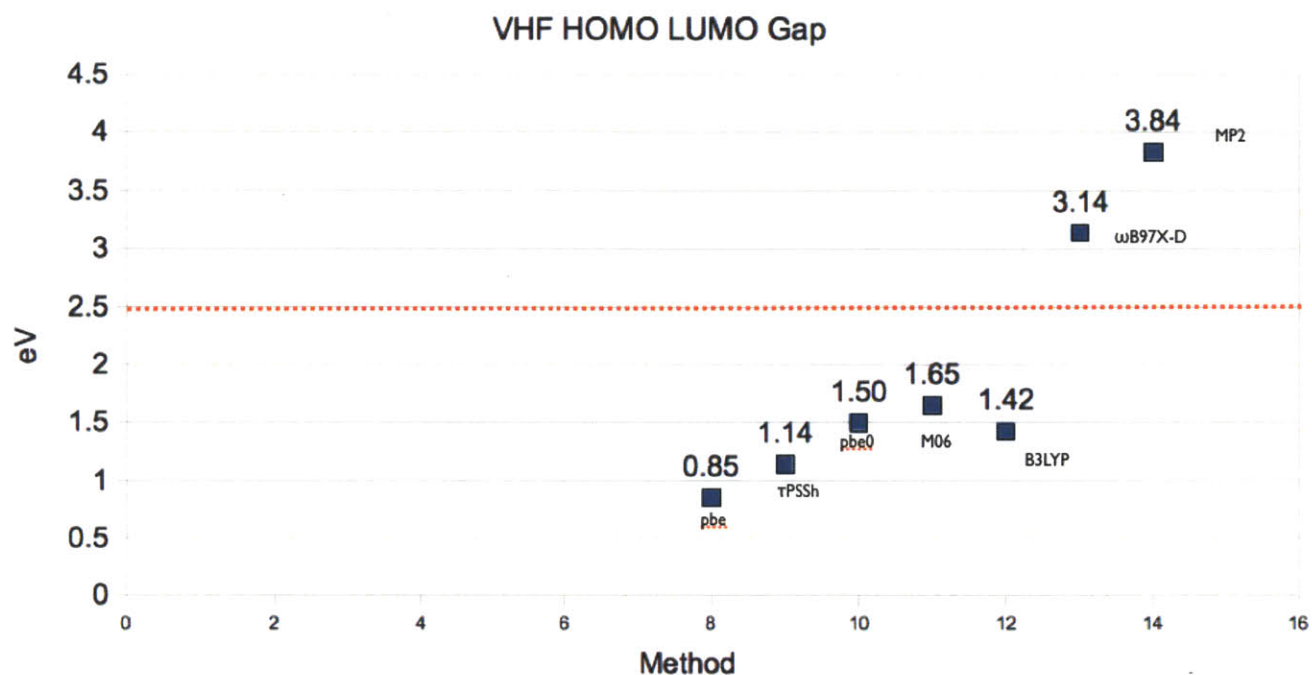


Figure 14. Calculated HOMO, LUMO gap for VHF

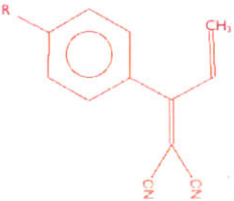
4. Conclusions, Further Discussions and Future Work

We calculated energy eigenvalues for DHA and VHF using the DFT Functionals: B3LYP, PBE, PBE0, M06, ω B97X-D, and τ PSSh and the post-HF methods: CCSD and MP2. Enthalpy calculations obtained from these energy eigenvalues indicated that all methods except B3LYP predict the correct sign for the enthalpy of the VHF DHA thermal back reaction. The ω B97X-D DFT Functional predicts a similar enthalpy value as the more computationally intense post Hartree-Fock methods: CCSD and MP2. HOMO LUMO gap values obtained from these eigenvalues indicated that the post Hartree-Fock Methods and the ω B97X-D Functional overestimate the HOMO LUMO gap, while the other DFT Functional Methods underestimate the HOMO LUMO gap. We compared the correlation energy, exchange energy, and kinetic and potential energy contributions to the energy for all of the DFT

Functionals. This comparison showed that the potential and kinetic energy contributions for each method differed. We compared the calculated structures for the DFT Functionals and CCSD for DHA and VHF. Comparison of the calculated DHA structures with the experimental structure showed that all methods predict the experimental geometry reasonably closely. Comparison of the out of plane distance for the calculated VHF structures indicated that the ω B97X-D Functional predicts a significantly different geometry from the other methods. We compared the calculated charge distribution for the B3LYP, PBE, PBE0, ω B97X-D, and τ PSSh Functional and CCSD calculations on DHA and VHF. All of these methods showed the effect of two strong electron withdrawing CN groups on the five-membered cyclic ring in DHA on the conjugation of the system. Interestingly, all functionals also showed little effect of the CN group on the phenyl ring on conjugation in DHA. All methods seem to suggest that the molecular orbitals present in DHA are largely delocalized across the entire molecule. In contrast, in VHF, all methods showed that the CN group on the phenyl ring affected the conjugation of the system in some way, and the the molecular orbitals were only delocalized across the phenyl ring and the two adjacent CN group. We hypothesize that the ω B97X-D functional, CCSD, and MP2 methods better account for weak interactions like van der Waals interactions, and pi-pi interactions, which is why they all give similar predictions, which are closer to experimental values. All of these conclusions along with other observations, hypotheses that might explain these observations, and further work that can be carried out to test or gain insight on these hypotheses are summarized in Table 5.

Table 5: Summary of Conclusions Based on the Observations On the Calculations

| Observation | Hypothesis | Further work that would lead further insight on hypothesis |
|--------------------------------|--|--|
| ω B97X-D functional and | ω B97X-D functional partitions the Hamiltonian that | CCSD calculations for a more complete basis should also predict a similar ΔH |

| | | |
|--|--|--|
| CCSD predict similar ΔH (Figure 7) | CC terms are included for certain distances between electrons | |
| B3LYP gives wrong sign for enthalpy calculation (Figure 7) | B3LYP accounts for electron correlation using both the LYP functional and an empirically fitted term. This empirically fitted term might be designed for molecules that are quite different from DHA and VHF | Literature search on what systems were used to fit B3LYP functional See how LYP functional calculations on the system compare with other functionals. If this functional gives a more accurate calculation of the enthalpy than the empirical fitted term is probably not suited to this system. |
| Each of the functionals had showed different potential and kinetic energy contributions to the energy calculation (Figure 8) | Each of the functionals is predicting different structures for DHA | They all seem to predict the experimental structure according to Table 3 Perform SP calculations to check that the deviations between calculated structure and experimental structure are not that large |
| | Each of the functionals is predicting different structures for VHF | Table 4 shows that ω B97X-D predicts a different geometry. Find another way to compare the structure to explain the difference between the kinetic and potential energy contributions for the other functionals Perform Relaxed Structure Calculations and SP Calculations for the methyl VHF derivative for which a published experimental structure is published |
| ω B97X-D functional predicted a significantly different out-of plane distortion from the other methods (Table 4) | This functional is accounting for an attractive interaction between the two CN groups and the seven-membered ring. | Calculate the structures and energies for  with each of the methods. If this hypothesis is correct, you expect the distance between the analogous carbons as compared in table 4 to be the same for all methods including ω B97X-D . |
| Large charge distribution about the CN groups attached to the phenyl ring for all | Due to the fact that CN is a strong electron withdrawing group, it significantly effects the conjugation in VHF. This same CN group does not | Carry out calculations on the Br derivative of the DHA/VHF system. Since Br is a less strong electron withdrawing group, each of the methods studied should give closer energy predictions to each other. Performing |

| | | |
|---|--|---|
| <p>methods visualization of VHF (Figures 11 and 12). Each method shows this effect to different degrees</p> | <p>effect the conjugation in DHA as significantly due to the fact that there is conjugation across the entire molecule. Due to the difference in the conjugation in DHA and VHF, error cancelation does not work so well</p> | <p>calculations on this variant of DHA/VHF has the added benefit that much experimental data has also been collected for this system[9].</p> <p>Carry out calculations on the CH₃ derivative of the DHA/VHF system. Since CH₃ is an even less strong electron withdrawing group than Br, the calculations for energies for each of the methods should agree most for this system.</p> |
|---|--|---|

5. Future Work

The most exciting result of this study is that it appears as though the ω B97X-D functional gives very similar predictions as the more computationally intensive post-HF CCSD and MP2 methods for this system. CCSD and MP2, and other similar post Hartree-Fock methods are generally considered superior at modeling weak interactions. It will be interesting to observe if this trend holds once CCSD calculations have been performed on the system for larger basis sets that include more polarization and diffuse functions like 6-311++ G(2d,d,p) or aug-cc-pVTZ. It appears as though all methods except B3LYP predict at least the correct sign for the enthalpy of the VHF DHA thermal back reaction. It would be interesting to further investigate why B3LYP fails to model this system, as B3LYP is a fairly standard DFT Functional used for organic molecules. One suggested calculation is to compare B3LYP's performance with the LYP functionals performance. Another interesting observation is that despite the fact that PBE, PBE0, and τ PSSh are parametrized in a similar manner, all three of these functionals give quite different predictions for this system. Future work could interrogate why these differences in the parametrization of the Functionals resulted in quite different predictions. It might be useful also to obtain experimental measurements for the enthalpy of this system. Another interesting avenue to pursue would be to conduct this same analysis on the methyl and Br derivatives of the DHA and VHF system, and compare the conclusions for the analysis of those systems to these ones.

References

- [1] *Acc. Chem. Res. Special Issue: Artificial Photosynthesis and Solar Fuels* **2009**, *42*, 1859–2029.
- [2] N.S Lewis, D.G. Nocera. “Powering the Planet: Chemical Challenges in the Solar Energy Utilization” *Proc. Natl. Acad. Sci.* **2006**, *103*, 15729–15735.
- [3] M. Kenisarin, K. Mahkamov. “Solar energy using Phase Change Materials” *Renew. Sust. Energ. Rev.* **2007**, *11*, 1913–1965.
- [4] A. J. Nozik, J. Miller. “Toward designed singlet fission: Electronic states and photophysics of 1,3-diphentlisobenzofuran”. *J. Chem. Rev.* **2010**, *110*, 6443–6445.
- [5] Alexei Kolpak, Jeffrey C. Grossman. “Azobenzene-Functionalized Carbon Nanotubes as High Energy Density Solar Thermal Fuels”. *Nano Lett.* 2011, *11*, 3156-3162.
- [6] J. Cho, L. Berbil-Bautista, I.V. Pechenezgshiy, N. Levy, S. K. Meir, S. Varadarajan, Y. Kanai, J.C. Grossman, K.P.C. Vollhardt, M.F. Crommie. “Single-molecule-resolved structural changes induced by temperature and light in surface-bound organic molecules designed for energy storage”. *ACS Nano*. Vol. 5 Iss. 5 May 24, 2011
- [7] L. Edjlali, E. Vessaly, M. Abbasian. “Solar energy absorption in norbornadiene- quadricyclane system through electron donating or withdrawing substituents”. *Russian Journal of Physical Chemistry* Vol. 85 No. 5 2011. 816- 820
- [8] Oleg Kushnir. “Molecular Switches Based on Dihydroazulene/Vinylheptafulvene Photochromism”. Dissertation, Dept. Chemie und Pharmazie, der Universität Regensburg, 2005.
- [9] S. L. Broman, M.A.Petersen, C.G. Tortzen, A. Kadziola, K. Kilsa, M.B. Nielsen. “Arylethynyl Derivatives of the Dihydroazulene/ Vinylheptafulvene Phot/Thermoswitch: Tuning the Switching Event”. *J. Am. Chem. Soc.* 2010, *132*, 9165-9174.

- [10] J. Daub, S. Gierisch, U. Klement, T. Knochel, G. Maas, U. Seitz. "Lichtinduzierte reversible Reaktionen: Synthesen und Eigenschaften photochromer 1,1-Dicyan-1,8a-dihydroazulene und thermochromer 8-(2,2-Dicyanvinyl)heptafulvene". Chem. Ber. 1986. 2631-2645.
- [11] M. Kaforty, M. Botoshansky, J. Daub, C. Fischer, A. Bross. "2-p-Cyanophenyl-1,8a-dihydroazulene-1,1-dicarbonitrile and Methyl 1-Cyano-2-p-cyanophenyl-1,8a-dihydroazulene-1-carboxylate". Acta Cryst. (1997). C53, 1665-1667.
- [12] H. Goerner, C. Fischer, S. Gierisch, and J. Daub. "Dihydroazulene/Vinylheptafulvene Photochromism: Effects of Substituents, Solvent, and Temperature in the Photorearrangement of Dihydroazulenes to Vinylheptafulvenes". J. Phys. Chem. 1993, 97, 4110-4117
- [13] Parker Cr et. al "Lewis acid enhanced switching of the 1,1-dicyanodihydroazulene/vinylheptafulvene photo/thermoswitch". Chem Commun (Camb) 2011 Jun 7; E pub 2011 Apr 18.
- [14] Martial Boggio-Pasqua et al. "Dihydroazulene/Vinylheptafulvene Photochromism: A Model of One-Way Photochemistry via a Conical Intersection". J. Am. Chem. Soc. Vol 124, No. 7, 2002, 1456-1469
- [15] Aurelie Plaquet, Benoit Champagne, Frederic Castet et. al "Theoretical investigation of the dynamic first hyperpolarizability of DHA-VHF molecular switches". New J. J. Chem., 2009, 33, 1349-1356.
- [16] Gaussian 09, Revision A.1, M. J. Frisch, G. W. Trucks, H. B. Schlegel, G. E. Scuseria, M. A. Robb, J. R. Cheeseman, G. Scalmani, V. Barone, B. Mennucci, G. A. Petersson, H. Nakatsuji, M. Caricato, X. Li, H. P. Hratchian, A. F. Izmaylov, J. Bloino, G. Zheng, J. L. Sonnenberg, M. Hada, M. Ehara, K. Toyota, R. Fukuda, J. Hasegawa, M. Ishida, T. Nakajima, Y. Honda, O. Kitao, H. Nakai, T. Vreven, J. A. Montgomery, Jr., J. E. Peralta, F. Ogliaro, M. Bearpark, J. J. Heyd, E. Brothers, K. N. Kudin, V. N. Staroverov, R. Kobayashi, J. Normand, K. Raghavachari, A. Rendell, J. C. Burant, S. S. Iyengar, J.

Tomasi, M. Cossi, N. Rega, J. M. Millam, M. Klene, J. E. Knox, J. B. Cross, V. Bakken, C. Adamo, J. Jaramillo, R. Gomperts, R. E. Stratmann, O. Yazyev, A. J. Austin, R. Cammi, C. Pomelli, J. W. Ochterski, R. L. Martin, K. Morokuma, V. G. Zakrzewski, G. A. Voth, P. Salvador, J. J. Dannenberg, S. Dapprich, A. D. Daniels, Ö. Farkas, J. B. Foresman, J. V. Ortiz, J. Cioslowski, and D. J. Fox, Gaussian, Inc., Wallingford CT, 2009.

[17] Humphrey, W., Dalke, A. and Schulten, K., "VMD - Visual Molecular Dynamics", *J. Molec. Graphics*, 1996, vol. 14, pp. 33-38.

[18] P. Hohenberg, W. Kohn. "Inhomogeneous Electron Gas". *Phys. Rev.* 136, B864-B871 (1964).

[19] Ira N. Levine. *Quantum Chemistry*. New York: Pearson Education Inc, 5th Ed, 2007.

[20] S.N. Pieniazek, F.R. Clemente, and K.N. Houk. "Sources of Error in DFT Computations of C-C Bond Formation Thermochemistries: $\pi \rightarrow \sigma$ Transformations and Error Cancellation by DFT Methods". *Angew. Chem. Int. Ed.* 2008, 47, 7746-7749.

[21] J. P. Perdew, K. Burke, and M. Ernzerhof, "Generalized gradient approximation made simple," *Phys. Rev. Lett.*, **77** (1996) 3865-68.

[22] C. Adamo and V. Barone, "Toward reliable density functional methods without adjustable parameters: The PBE0 model," *J. Chem. Phys.*, **110** (1999) 6158-69.

[23] A. D. Becke, "Density-functional thermochemistry. III. The role of exact exchange," *J. Chem. Phys.*, **98** (1993) 5648-52.

[24] Christopher J. Cramer. *Essentials of Computational Chemistry: Theories and Models*. USA: Wiley, 2nd Ed. 2004.

[25] J. M. Tao, J. P. Perdew, V. N. Staroverov, and G. E. Scuseria, "Climbing the density functional ladder: Nonempirical meta-generalized gradient approximation designed for molecules and solids,"

Phys. Rev. Lett., **91** (2003) 146401.

[26] J.-D. Chai and M. Head-Gordon, "Systematic optimization of long-range corrected hybrid density functionals," *J. Chem. Phys.*, **128** (2008) 084106.

[27] J.-D. Chai and M. Head-Gordon, "Long-range corrected hybrid density functionals with damped atom-atom dispersion corrections," *Phys. Chem. Chem. Phys.*, **10** (2008) 6615-20.

Acknowledgements

I would like to thank Professor Grossman for advising me and giving me this opportunity ; Dr. Alexie Kolpak who spent many hours teaching me, proof reading my thesis, showing me how to run calculations, and encouraging me; Dr. Tim Kucharski who showed me how to use experimental equipment; and the rest of the Grossman group who were always happy to take time from their work and answer my questions. I have learnt a lot from all of you. I have also enjoyed getting to know all of you very much.